analytical chemistry

pubs.acs.org/ac Article

Novel Porphyrin Zr Metal–Organic Framework (PCN-224)-Based Ultrastable Electrochemiluminescence System for PEDV Sensing

Jing Ma, Wenjing Wang, Yun Li, Zhicheng Lu, Xuecai Tan, and Heyou Han*

Cite This: *Anal. Chem.* 2021, 93, 2090–2096 Read Online

ACCESS | Metrics & More | Article Recommendations | Supporting Information

ABSTRACT: The sensitive detection of coronavirus is of vital importance for the prevention of its rapid spread. Porcine epidemic diarrhea virus (PEDV) is a highly contagious coronavirus that causes severe diarrhea and death in neonatal piglets. In this work, a novel PCN-224-based electrochemiluminescence (ECL) system was constructed for PEDV detection with high sensitivity. We found that PCN-224 can be employed as an ECL reporter with a strong signal because of its zirconium-based organic porous frame nanomaterial with a large specific surface area and stable structure. TiO_2 nanoparticles were used as an accelerator for the first time to promote the reduction of coreactant potassium peroxydisulfate on the cathode; thus, the initial ECL signal of PCN-224 was significantly amplified. In the presence of PEDV, the ECL signal decreased due to the block effect to electron transfer. As a result, the novel "signal off" biosensor achieved a sensitive detection of PEDV ranging from 1 pg/mL to 10 ng/mL, with a detection limit of 0.4 pg/mL (S/N = 3). Importantly, the PCN-224 nanomaterial enriched the ECL system in biological analysis, and the proposed strategy provided a new route for coronavirus detection.

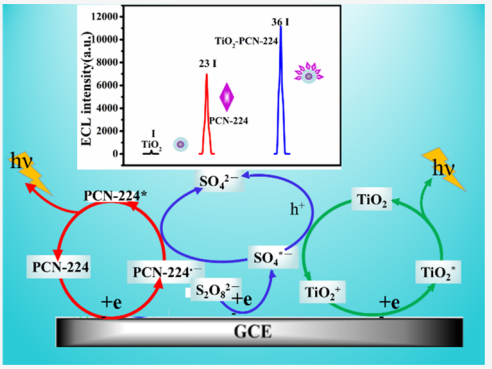

INTRODUCTION

Porcine epidemic diarrhea virus (PEDV) is a linear single-stranded RNA virus, its nucleic acid molecules are infectious, and symptoms of PEDV infection are vomiting, diarrhea, and dehydration.[1] The high incidence rate and mortality cause extremely serious harm in the herd.[2] By clinical symptom observation, it is very difficult to discriminate PEDV infection with transmissible gastroenteritis (TGE); therefore, laboratory diagnosis is needed. At present, the main laboratory diagnostic methods include enzyme-linked immunosorbent assay (ELISA), immunoelectron microscopy, immunofluorescence assay (IFA), reverse-transcription polymerase chain reaction (RT-PCR), and so on.[3−5] However, new methods are needed to overcome the shortcomings of these methods, such as complex equipment, time-consuming, and tedious operations.[6]

Electrochemiluminescence (ECL) combines the advantages of electrochemistry and chemiluminescence and is an important analysis method with merits of high sensitivity, low background, and fast and simple detection process.[7] It has been widely used in biological immune analysis, medical diagnosis, and food and environmental monitoring and has become one of the important methods of in vitro diagnosis.[8−13] ECL luminaries play an important role in ECL analysis.[6,14−19] For example, our group used quantum dots, $Ru(bpy)_3^{2+}$ as luminaries to detect the virus. Furthermore, different materials including metal complexes (iridium complexes),[20,21] aromatic organic compounds (fluorene, anthracene, perylene, benzooxazole derivatives, and phenothiazine), and nanoparticle complexes have been reported as effective ECL luminaries.[9,22−26] However, these materials are toxic or coreactants are harmful to the environment.[27] Based on this motivation, we want to seek nontoxic and environmentally friendly materials.

Although the first report of porphyrins ECL by Bader dates back to 1972, there had been rare research on the ECL of porphyrins.[28−30] Porphyrinic Zr metal–organic framework (MOF) PCN-224 is a kind of porous structure nanomaterial that is composed of Zr_6 cluster and TCPP with good biocompatibility and excellent stability in a physiological environment, where porphyrins are used for light harvesting as well as in energy and electron transfer.[31−33] In recent years, PCN-224 has been used in a photo-electrochemical sensor, fluorescence sensor, photodynamic therapy, and so on.[31,34,35] However, the ECL property of PCN-224 has never been studied previously.

At the same time, nano-TiO_2 was widely used in the construction of a biosensor, photocatalyst, and battery because of its stable conductivity and long-term chemical stability.[27,36] It was also used as a fixed material in ECL due to its good film-forming performance and low toxicity.[37] For example, nano-

Received: September 9, 2020
Accepted: January 5, 2021
Published: January 13, 2021

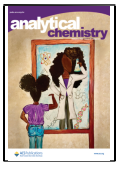

https://dx.doi.org/10.1021/acs.analchem.0c03836
Anal. Chem. 2021, 93, 2090–2096

TiO_2 had been reported to be able to immobilize probes and could also promote the reduction of dissolved O_2 due to the oxidizing nature of the holes generated in TiO_2, thus enhancing the ECL intensity of cathode silver clusters.[38]

Based on the abovementioned background, the zirconium-based MOF nanoparticles PCN-224 with a porphyrin ring were synthesized. We tested the stability and studied the ECL mechanism and properties in potassium persulfate solution. Furthermore, PCN-224 was employed to construct an ECL biosensor to detect PEDV. As illustrated in Scheme 1, the ECL

Scheme 1. (A) Schematic Diagram of the Synthesis Process of PCN-224; (B) Schematic Representation of Working Principle for the Signal-off ECL Sensing Platform

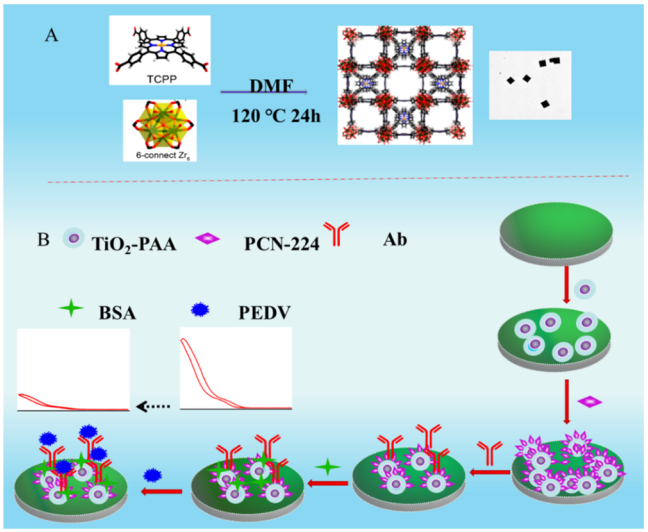

intensity of PCN-224 could be greatly enhanced by the electrostatic adopted TiO_2, which was modified with polyacrylic acid (PAA). PEDV antibody was conjugated with PCN-224 by virtue of amide-carboxyl conjugation, and PEDV antibody specifically recognizes antigen. With the increase in PEDV, the ECL signal gradually decreases due to the steric hindrance effect caused by protein molecules.

EXPERIMENTAL SECTION

Preparation of PCN-224. The synthesis of PCN-224 was based on the method reported by Feng's groups,[39] which is described in the Supporting Information.

Construction of a Label-free ECL Immunosensor. The glassy carbon electrode was polished with 0.3 and 0.05 μm aluminum oxide powder, respectively, then underwent ultrasonication for 1 min in nitric acid aqueous solution (V_{HNO_3}/V_{H_2O} = 1:1) and water, and finally blow-dried with N_2. Then, 6 μL of 0.5 mg/mL TiO_2–PAA composite was dropped on the glassy carbon electrode and dried at room temperature. After washing by dipping in phosphate-buffered saline with 0.02% Tween 20 (PBST, pH 7.4, 0.02 M NaH_2PO_4, 0.02 M Na_2HPO_4, 0.9% NaCl) solution three times, 6 μL of 1 mg/mL activated PCN-224 was taken to drop on the electrode and placed in the dark. After an hour, the modified electrode was gently washed, and 10 μL 1 mg/mL Ab_1, diluted 1000 times, was dropped on the electrode and incubated at 37 °C for 1 h to obtain Ab_1/PCN-224/TiO_2. In order to block the nonspecific binding site, 6 μL of 0.5% BSA was dropped on the electrode and incubated at 37 °C for 0.5 h. Finally, after PBST washing, PEDV was dropped on the label-free ECL immunosensor and incubated at 37 °C for 1 h for target identification.

Detection of PEDV. Before detection, the abovementioned electrode was first dipped in PBST solution and then stored away from light at 4 °C. In the MPI-EII ECL device, a homemade 10 mL electrolytic cell and a three-electrode system were used. The reference electrode is the saturated Ag/AgCl electrode filled with potassium chloride, the working electrode is the modified GCE electrode, and the counter electrode is the Pt wire. The ECL test condition was 0.05 M $K_2S_2O_8$ solution with a scanning voltage of −1.2 to 0 V, PMT-800 V, and a scanning speed of 0.3 V/s.

RESULTS AND DISCUSSION

Choice of Materials. In our study, PCN-224 has six edges connecting to carboxylates from TCPP and was employed as an ECL emitter, where porphyrins are used for light harvesting as well as in energy and electron transfer.[31−33] TiO_2 nanoparticles were used as a fixed material on the electrode in the ECL study due to its good film-forming performance, stable conductivity, long-term chemical stability, and low toxicity.[27,36] The combination of the two materials produces a stronger ECL signal because TiO_2 has a wide band gap and PCN-224 has a relatively small band gap, therefore generating a lot of electron−hole complex bonding.

Characterization of PCN-224. Transmission electron microscopy (TEM) image and scanning electron microscopy (SEM) image of PCN-224 are shown in Figure 1A; the

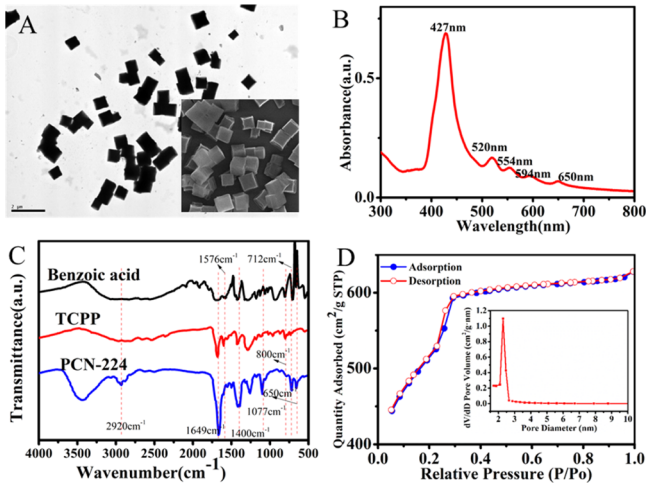

Figure 1. (A) TEM image of PCN-224 (the inset is the SEM image of PCN-224); (B) UV−vis absorption spectra of PCN-224; (C) FT-IR spectra of benzoic acid, TCPP, and PCN-224; and (D) N_2 adsorption−desorption isotherm of PCN-224 at 77 K (the inset is the pore size distribution graph).

product is cubic in shape with good dispersity. As can be seen from Figure S1, the average diameter is 480 nm. Meanwhile, the UV−vis spectra (Figure 1B) of PCN-224 show that PCN-224 has a major S peak (427 nm) and four Q bands (520, 554, 594, and 650 nm), which is mainly caused by the electron−hole separation ability and photon absorption of PCN-224 under light radiation.[31] It can be observed from the Fourier infrared spectra of PCN-224 (Figure 1C) that there are symmetric and asymmetric stretching vibration peaks of the

https://dx.doi.org/10.1021/acs.analchem.0c03836
Anal. Chem. 2021, 93, 2090−2096

COO^- group at 1400 cm^{-1} and 1649 cm^{-1}, respectively. The C−H bond peak of the benzene and pyrrole ring appearing at 2920 cm^{-1}, 1576 cm^{-1} is the vibration peak of the C═C elongation functional group of phenyl and pyrrole, and the deformation peak of pyrrole appears at 1077 cm^{-1}.The C−H peak of phenyl out-of-plane binding is also observed at 712 and 800 cm^{-1} and the vibration peak of Zr−OH is at 650 cm^{-1}, which also indicates the successful synthesis of PCN-224.[40]

Figure 1D shows the N_2 adsorption isotherm of PCN-224, a reversible type-I adsorption behavior was observed, indicating that the material has microporous characteristics. The pore diameter is centered at about 2.8 nm. TGA was performed on the prepared PCN-224, as shown in Figure S2. PCN-224 is relatively stable among MOF material in terms of weight loss at different temperatures.

ECL Study. The current density was calculated by referring to the method of Hasan Bagheri' group,[41,42] which was described in the Supporting Information. In Figure 2A, there is

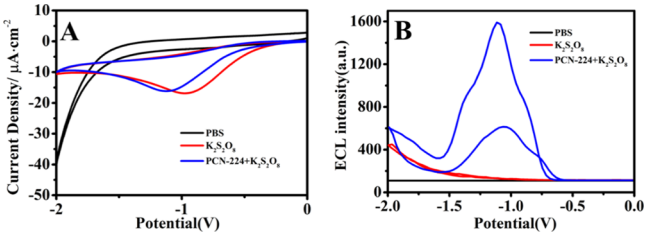

Figure 2. CV (A) and ECL intensity−potential curves (B) of a bare GCE in 10 mM pH 7.4 PBS (black curve), 0.05 M $K_2S_2O_8$ (red curve), and 0.16 mg/mL PCN-224 + 0.05 M $K_2S_2O_8$ (blue curve). Scan rate: 0.3 V/s.

no distinct oxidation−reduction peak in PBS solution and a visible reduction peak at −0.9 V is observed in $K_2S_2O_8$ solution. When PCN-224 was added, the peak position shifts to −1.1 V. $K_2S_2O_8$ can be reduced when scanning from −0.8 V to a more negative potential, and there is an obvious reduction peak at −0.9 V, which is attributed to $S_2O_8^{2-}$ reduction producing $SO_4^{\bullet-}$. At the same time, $OH^{\bullet}$ may also be produced in the reaction process, and $OH^{\bullet}$ will increase the number of $SO_4^{\bullet-}$ near the electrode by reducing $S_2O_8^{2-}$ to $SO_4^{\bullet-}$.[43] When PCN-224 was added into the solution, the reduction peak of $PCN\text{-}224^{\bullet-}$ appeared at −1.1 V due to the electron injection. Light emission occurred when $PCN\text{-}224^{\bullet-}$ is combined with $SO_4^{\bullet-}$.[44] In Figure 2B, the ECL signal was generated at −0.9 V in $K_2S_2O_8$ solution, and when PCN-224 was added, the ECL signal was generated at −0.6 V and reached the maximum value at −1.1 V, while no ECL was generated in PBS solution.

In order to obtain the maximum ECL strength of PCN-224 in $K_2S_2O_8$ solution, the main conditions including potential window, scan rate, pH, and concentration of $K_2S_2O_8$ were optimized. In Figure S3A, ECL intensity of PCN-224 was the highest when the scanning potential ranged from 0 to −1.2 V. If the potential was less than −1.2 V, hydrogen evolution reaction would occur, which made porphyrin rings in PCN-224 easily protonated and affected the ECL of PCN-224.[45] Figure S3B shows that ECL intensity reaches its maximum value at 0.3V·s^{-1}, which is due to the rapid formation of PCN-224*. However, when the scanning rate is greater than 0.3V·s^{-1}, the ECL intensity began to decline as the electrochemical reaction of $S_2O_8^{2-}$ could not keep up with the scanning rate.[46] When the $K_2S_2O_8$ concentration increases, the ECL intensity also increases, as shown in Figure S3C. It reaches the maximum value at 0.05 M. The further increase in $K_2S_2O_8$ leads to the decrease in ECL intensity, since under the circumstance of high concentration of $S_2O_8^{2-}$, the $SO_4^{\bullet-}$ is excessive and the free radicals are less. As shown in Figure S3D, the effect of pH on ECL strength is not great, which is due to the strong stability of its structure whether in acid or base solutions.[39] Therefore, the optimal pH value is 7.4. In summary, the optimal parameters of the proposed ECL biosensor are 0 to −1.2 V, 0.3 V·s^{-1}, 0.05 M $K_2S_2O_8$, and pH 7.4.

Characterization of TiO_2-PAA. First, its morphology was observed under TEM, as shown in Figure S4A, TiO_2 nanoparticles present relatively uniform size, and the maximum UV absorption peak occurs at 346 nm (Figure S4B). As the adhesion of PCN-224 to the electrode is relatively weak, it easily falls off during the process of biosensor construction and it is urgent to find a method to fix it. Considering that TiO_2 and PCN-224 are both positively charged, PAA, a polyanionic electrolyte, was employed. After being modified with PAA, TiO_2 can change its charge and become negatively charged, thus having a good adsorption effect on PCN-224. As can be seen from Figure S4C, the charge of unmodified TiO_2 nanoparticles is +29 mV, and the composite is negatively charged after modification.[47] The zeta potential of PCN-224 and TiO_2−PCN-224 is +37 mV and +12 mV, respectively, so TiO_2-PAA can easily combine with PCN-224 due to electrostatic interaction.

As shown in Figure S4D, the strong broad band near 400−800 cm^{-1} of TiO_2 powder belongs to Ti−O vibration, while the Ti−OH vibration peak appears at 2335 cm^{-1}. When modified with PAA, a wide band was shown at 3400 cm^{-1} for the TiO_2-PAA sample, which is related to the hydroxyl group on the surface and is caused by O−H stretching. The asymmetric stretching vibration peak of $-CH_3$ appears at 2967 cm^{-1}. There are symmetric and asymmetric stretching vibration peaks of the COO group at 1432 cm^{-1} and 1641 cm^{-1}, respectively. The weak band at 1245 cm^{-1} represents the deformation vibration peak of CH_2,[48,49] indicating that PAA has been successfully adsorbed on TiO_2.

ECL Enhancement Mechanism Study for TiO_2−PCN-224. Figure 3A,B shows the ECL and CV profiles of TiO_2 nanoparticles, PCN-224, and TiO_2−PCN-224 in 0.05 M $K_2S_2O_8$ solution. The ECL behavior of TiO_2 starts from −1.0 V, while that of PCN-224 and TiO_2−PCN-224 starts from −0.5 V. In addition, as can be seen from Figure 3A, for the TiO_2−PCN-224 sample, the more negative the potential is, the greater its ECL intensity will be. When it reaches −1.1 V, the maximum value will be achieved. In $K_2S_2O_8$ solution, the ECL intensity of TiO_2 is 309 a.u. and PCN-224 is 6969 a.u., while the ECL intensity of TiO_2 combined with PCN-224 is 1.6 times greater than that of PCN-224 (the ECL intensity increases from 6969 a.u. to 11,166 a.u.), 36 times greater than that of TiO_2 ECL intensity.

On the electrode surface due to the reduction effect of $K_2S_2O_8$, the cathode reduction current peak will appear when the scanning potential reaches −0.8 V in all the test processes. It can be seen from Figure 3B that the current density generated by PCN-224 and TiO_2−PCN-224 is much greater than that generated by TiO_2 mainly because TiO_2 nanoparticles are not only used as the fixed probe but also for good electron transfer capability.[27,50] The introduction of PCN-224 can improve electron transfer.

https://dx.doi.org/10.1021/acs.analchem.0c03836
Anal. Chem. 2021, 93, 2090−2096

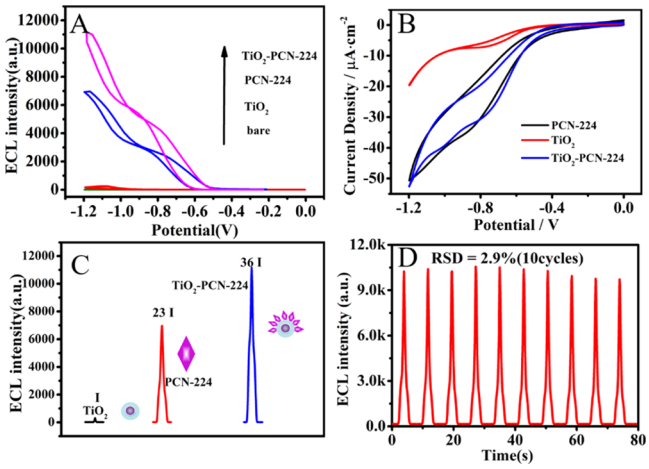

Figure 3. (A) ECL potential curves of TiO_2, PCN-224, and TiO_2−PCN-224; (B) CV of TiO_2, PCN-224, and TiO_2−PCN-224; and (C) ECL time curves of TiO_2, PCN-224, and TiO_2−PCN-224 (0.1 M, pH 7.4, 0.05 M $K_2S_2O_8$). (D) Stability of TiO_2−PCN-224 under consecutive 10 cyclic potential scans (−1.2 to 0 V, 0.3 V/s).

After coupling of TiO_2 and PCN-224, the improvement of ECL efficiency may be due to the following mechanisms shown in Supporting Information eqs S1−S8.[44,S1] From Supporting Information reactions 1 and 2, $S_2O_8^{2-}$ can obtain an electron from the electrode. TiO_2 can fix h^+ in Supporting Information eqs S3 and S4 and PCN-224 can also directly obtain an electron from the electrode (Supporting Information eq S6). Due to the combination of TiO_2 with a wide band gap and PCN-224 with a relatively small band gap, it is easier for e^- to transfer from PCN-224 to TiO_2, thus generating a lot of electron−hole complex bonding. Then, TiO_2* will also be produced when PCN-224 (e^-) is combined with TiO_2 (h^+) (Supporting Information eq S7).

On the other hand, the combination of TiO_2 and PCN-224 can make it easier for h^+ in Supporting Information eq S7 to transfer from the TiO_2 valence band to PCN-224, thus making it easier to form PCN-224*, as shown in Supporting Information eq S8, so PCN-224* will emit light. At this time, the ECL intensity of the TiO_2−PCN-224-modified electrode will be greater than that of TiO_2- and PCN-224-modified electrode alone.

What else, it can be seen from Figure 3D that the TiO_2−PCN-224-modified electrode can maintain a stable ECL emission when a photomultiplier tube is set at 800 V, with an RSD of 2.9%. The stable structure of TiO_2−PCN-224 and its strong ECL signal in $K_2S_2O_8$ solution indicate that TiO_2−PCN-224 can be used in subsequent biosensor applications. In conclusion, as a new ECL nanoprobe, TiO_2−PCN-224-$K_2S_2O_8$ is ultrastable with high ECL intensity. Compared with quantum dots, it is toxic element-free; Compared with $Ru(bpy)_3^{2+}$, the coreactant is environmentally friendly, indicating that it can be further used in biosensing.

Feasibility Analysis of ECL PEDV Sensing. The construction process of the PEDV sensor was verified by cyclic voltammograms (CVs) and electrochemical impedance spectroscopy (EIS) in 0.1 M KCl and 5 mM $K_3Fe(CN)_6$ electrolyte solution.

As shown in Figure 4A, compared with the bare electrode (curve a), the CV peak current of the TiO_2-modified electrode (curve b) was significantly weakened, the reason is that the negatively charged surface made $[Fe(CN)_6]^{3-/4-}$ repulsive and

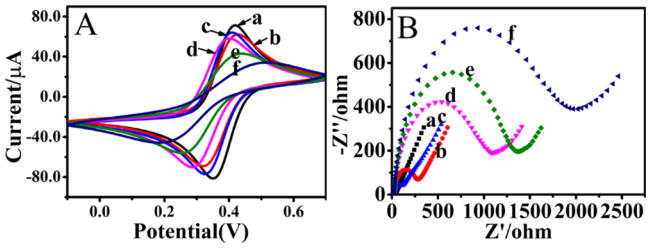

Figure 4. (A) CV and (B) impedance curves for different fabricated steps: (a) GCE; (b) TiO_2/GCE; (c) PCN-224/TiO_2/GCE; (d) Ab_1/PCN-224/TiO_2/GCE; (e) BSA/Ab_1/PCN-224/TiO_2/GCE; and (f) Ag/BSA/Ab_1/PCN-224/TiO_2/GCE in an electrolyte solution containing 0.1 M KCl and 5 mM $K_3Fe(CN)_6$. Scan rate: 100 mV/s.

prevented electron transfer.[52] When modified by PCN-224, the CV peak current (curve c) increased compared with curve b mainly because of the large surface area and excellent electron transfer acceleration capability of PCN-224. When Ab_1, BSA, and PEDV were successively incubated with PCN-224/TiO_2/GCE, the redox peak (curve d, e, and f) was successively decreased, which is due to the fact that protein is a nonconductive material and will seriously hinder the diffusion of $[Fe(CN)_6]^{3-/4-}$. The abovementioned results indicate that the PEDV ECL platform has been successfully constructed.

EIS is an electrochemical method to monitor the assembly processes of the electrode step-by-step. As shown in Figure 4B, the Nyquist curve of the impedance spectrum shows the different steps of biosensor construction. When TiO_2 is modified on the electrode, the impedance increased from 13.24 to 222 Ω (curve b); subsequently, after the modification of PCN-224 with good electrical conductivity, the impedance of the electrode decreased from 222 to 7.97 Ω (curve c). Then, protein molecules Ab_1, BSA, and PEDV were incubated with the electrode, and due to their poor conductivity, the impedance value increases continuously (curve d, R_{et} = 888 Ω; curve e, R_{et} = 1147 Ω; and curve f, R_{et} = 1556 Ω). The abovementioned experimental results are consistent with CV results, indicating the successful construction of the PEDV immunosensor.

To verify the construction process of the PEDV ECL sensor, changes in ECL intensity of glassy carbon electrodes were also characterized. As shown in Figure 5, when TiO_2 is modified on the electrode, its ECL strength is 180 a.u. When PCN-224/TiO_2/GCE was constructed, the measured ECL intensity increases to 13,705 a.u. When Ab_1, BSA, and PEDV were incubated with the electrode, their ECL intensity is 10,349 a.u., 7959 a.u., and 2991 a.u., respectively. With the adsorption of

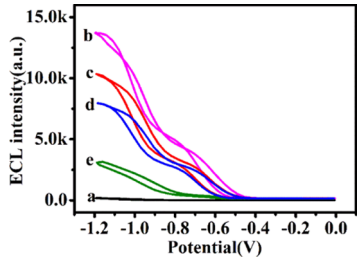

Figure 5. Cathodic ECL response for each immobilized step: (a) TiO_2/GCE (black); (b) PCN-224/TiO_2/GCE (pink); (c) Ab_1/PCN-224/TiO_2/GCE (red); (d) BSA/Ab_1/PCN-224/TiO_2/GCE (blue); and (e) Ag/BSA/Ab_1/PCN-224/TiO_2/GCE (green).

https://dx.doi.org/10.1021/acs.analchem.0c03836
Anal. Chem. 2021, 93, 2090−2096

protein, the steric resistance of protein molecules is increased due to its insulation, leading to the decrease in ECL intensity. The ECL results can also prove the successful construction of signal-off ECL PEDV immunosensor.

Optimization of Experimental Parameters. In order to achieve the best ECL response to PEDV detection, the amount of PAA that used to modify TiO_2, the amount of TiO_2, and the amount of PCN-224 were studied during the construction of the sensor. Specific results are shown in Figure S5. To optimize PAA amount, 0%, 1%, 2%, 3%, 4%, and 5% PAA were used to modify TiO_2, respectively, and zeta potential and ECL intensity were subsequently monitored. Figure S5A shows that when TiO_2 was not modified by PAA, its charge was +28 mV, and when different amounts of PAA were applied, its potential changed to about −24 mV. At this time, the corresponding ECL intensity was investigated. According to Figure S5B, TiO_2 modified with 2% PAA had the highest ECL intensity; therefore, 2% PAA was chosen to modify TiO_2. The amount of modified TiO_2 was also discussed. As displayed in Figure S5C, 4 μL of TiO_2 was chosen here for electrode modification. Finally, as shown in Figure S5D, when we varied PCN-224 concentration from 0.25 to 1 mg/mL, the ECL intensity increases with the increase in the dosage, but when the concentration reached above 1 mg/mL, excessive loaded PCN-224 would stop the spread of the electron transfer or prevent total reactant from the electrode surface; thus, the ECL intensity remained constant and decreased with the increasing concentration.[51]

Application of the ECL Immunosensor in PEDV Detection. Under optimal conditions, a signal-off ECL immunosensor was constructed to quantitatively analyze PEDV. As shown in Figure 6A, the ECL intensity on the electrode incubated with different concentrations of PEDV was measured, and the ECL intensity decreased with the increase in antigen concentration. The calibration plot was displayed in Figure 6B, there is a good linear relationship between the ECL intensity and the logarithm of PEDV concentration ranging from 1 pg/mL to 10 ng/mL. The linear equation is $I_{ECL} = -1531.86 \log C + 2474.17$, $R^2 = 0.9972$, and the measured detection limit is 0.4 pg/mL (S/N = 3). This result indicates that this method can be used to detect PEDV. The charge-transfer resistance of the proposed biosensor in the presence of varying PEDV was also investigated. Figure S6 displays the Nyquist curve of the impedance spectrum with different concentrations of PEDV. With increasing concentrations of PEDV, an increase in R_{ct} is observed, indicating that the electron transfer kinetics of the redox probe was hindered by the insulating property and steric hindrance effect of antigen, which contributed to the decreased ECL intensities.

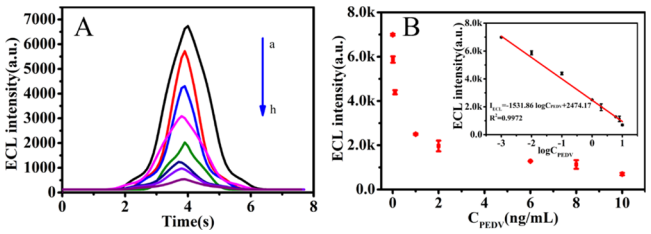

Figure 6. (A) ECL response of the proposed biosensor to PEDV with varying concentrations: (a) 0.001; (b) 0.01; (c) 0.1; (d) 1; (e) 2; (f) 6; (g) 8; and (h) 10 ng/mL in PBS (0.1 M, pH 7.4) containing 0.05 M $K_2S_2O_8$ with a scan rate of 300 mV/s. (B) Calibration plot of the ECL intensity with varying PEDV concentrations (The inset is linear relationship of ECL intensity vs logarithm of PEDV concentrations).

Specificity, Repeatability, and Stability of the ECL Platform. In order to verify the specificity of the method, five different proteins including BSA, IgG, PCV, PRRSV, EV 71, and TGEV were used as interference substances of PEDV to evaluate the accuracy of the method. As shown in Figure S7A, BSA (1 ng/mL), IgG (3 ng/mL), PCV (3 ng/mL), PRRSV (3 ng/mL), EV 71 (3 ng/mL), and TGEV (3 ng/mL) were used to replace the target for the comparative test. It can be observed that when these interferences replace PEDV, there is no significant change in the ECL signal. However, when they were added to PEDV (3 ng/mL) solution, the measured ECL intensity was close to that of PEDV (3 ng/mL) as the target object. Thus, BSA, IgG, PCV, PRRSV, EV 71, and TGEV have almost no effect on the ECL response of PEDV, indicating that the sensor has good selectivity and specificity. We also constructed the ECL immunosensors without Ab and with DF-C12C mAb (Huang-long-bing antibody). It can be observed in Figure S7B that there is no significant change in the ECL signal, demonstrating that our proposed biosensor exhibits good resistance against nonspecific adsorption.

The measured signal stability was also of great significance for the use of the sensor. For this reason, we investigated the stability of this signal-off sensor in $K_2S_2O_8$ solution with a PEDV concentration of 3 ng/mL and an electrolyte solution of 0.05 M and scanned the ECL intensity for 10 cycles continuously. As shown in Figure S8, there was no significant change in the ECL peak, with an RSD of 1.4%. It could be seen that the ECL sensor had good stability. At the same time, its repeatability was also investigated. Three groups of electrodes were constructed at the same time for each concentration, and the relative standard deviation was calculated as 2.1%. Furthermore, the ECL signal intensity of the same biosensor retained 94.2% of the original value after being stored at 4 °C for 1 week, which indicated that the sensor had a good reproducibility (data not shown).

In order to verify the feasibility of the ECL sensor in clinical application, pig manure was centrifuged for dilution, and PEDV with known concentration was added for standard recovery verification. The relative standard deviation and recovery rate of PEDV ECL immunoassay are listed in Table S1. It can be seen that the standard recovery rate of samples ranges from 94.0 to 110.0%, and the standard deviation of PEDV antibody (n = 3) is 1.5−7.2%. PEDV in swine faeces was adopted as real samples in the detection. The diluted samples (from pigs with clinical diarrhea) were analyzed using the proposed method (Table S2). As shown in the table, our proposed method exhibited high consistence with the standard ELISA method, suggesting the feasibility and selectivity of the proposed method. The abovementioned results show that the ECL sensor can be applied to the analysis and detection of actual biological samples.

CONCLUSIONS

In conclusion, an immunosensor based on a novel PCN-224/$K_2S_2O_8$/TiO_2 ternary ECL system with TiO_2-sensitized PCN-224 as a signal label for signal amplification was successfully constructed to PEDV. The constructed ECL sensor has the advantages of high affinity, good stability, high sensitivity, and wide linear range. The results show that this method not only broadens the application of PCN-224 in ECL but also can be extended to the development of quantitative detection of

https://dx.doi.org/10.1021/acs.analchem.0c03836
Anal. Chem. 2021, 93, 2090−2096

various viruses. Considering the fast spread speed of coronavirus, our proposed strategy owns great potential for wide applications. However, our proposed biosensing platform is the signal-off mode, the signal may be influenced by environmental changes for the detection of trace level analytes,[53] and the signal-on sensing mode using PCN-224 is under development.

■ ASSOCIATED CONTENT

Supporting Information

The Supporting Information is available free of charge at https://pubs.acs.org/doi/10.1021/acs.analchem.0c03836.

Materials and reagents; measurements; ECL detection mechanism on TiO_2−PCN-224 in $S_2O_8^{2-}$ solution; size distribution and TGA of PCN-224; optimization of ECL strength of PCN-224 in $K_2S_2O_8$ solution; characterization of TiO_2 NPs; optimization of experimental parameters; RCT of the proposed biosensor to PEDV; histogram for the specificity of this method for PEDV detection; stability of the proposed method; and recoveries of PEDV from the excrement detected by the proposed immunosensor (PDF)

■ AUTHOR INFORMATION

Corresponding Author

Heyou Han − *State Key Laboratory of Agricultural Microbiology, College of Food Science and Technology, College of Science, Huazhong Agricultural University, Wuhan 430070, People's Republic of China;* orcid.org/0000-0001-9406-0722; Email: hyhan@mail.hzau.edu.cn; Fax: (+86)-027-8728 8505

Authors

Jing Ma − *State Key Laboratory of Agricultural Microbiology, College of Food Science and Technology, College of Science, Huazhong Agricultural University, Wuhan 430070, People's Republic of China; College of Life Science, Yangtze University, Jingzhou, Hubei 434023, People's Republic of China*

Wenjing Wang − *State Key Laboratory of Agricultural Microbiology, College of Food Science and Technology, College of Science, Huazhong Agricultural University, Wuhan 430070, People's Republic of China;* orcid.org/0000-0003-4035-8552

Yun Li − *State Key Laboratory of Agricultural Microbiology, College of Food Science and Technology, College of Science, Huazhong Agricultural University, Wuhan 430070, People's Republic of China*

Zhicheng Lu − *State Key Laboratory of Agricultural Microbiology, College of Food Science and Technology, College of Science, Huazhong Agricultural University, Wuhan 430070, People's Republic of China*

Xuecai Tan − *College School of Chemistry and Chemical Engineering, Guangxi University for Nationalities, Nanning 530008, People's Republic of China*

Complete contact information is available at: https://pubs.acs.org/10.1021/acs.analchem.0c03836

Notes

The authors declare the following competing financial interest(s): J.M. and W.W. contributed equally to this work.

■ ACKNOWLEDGMENTS

This research was financially supported by the National Key R&D Program (2016YFD0500706), the National Natural Science Foundation of China (21778020 and 21804046), and Sci-tech Innovation Foundation of Huazhong Agriculture University (2662017PY042). We thank Dr. Zhonghua Li for providing PEDV antigen, antibody, and real samples. We thank Prof. Fang Ding for providing Huang-long-bing antibody.

■ REFERENCES

(1) Hanke, D.; Pohlmann, A.; Sauter-Louis, C.; Höper, D.; Stadler, J.; Ritzmann, M.; Steinrigl, A.; Schwarz, B.-A.; Akimkin, V.; Fux, R.; Blome, S.; Beer, M. *Viruses* **2017**, *9*, 177.

(2) Wang, D.; Fang, L.; Shi, Y.; Zhang, H.; Gao, L.; Peng, G.; Chen, H.; Li, K.; Xiao, S. *J. Virol.* **2016**, *90*, 2090−2101.

(3) Bigault, L.; Brown, P.; Bernard, C.; Blanchard, Y.; Grasland, B. *J. Virol. Methods* **2020**, *283*, 113906.

(4) Ren, X.; Suo, S.; Jang, Y.-S. *Biotechnol. Lett.* **2011**, *33*, 215−220.

(5) Zeng, S.; Zhang, H.; Ding, Z.; Luo, R.; An, K.; Liu, L.; Bi, J.; Chen, H.; Xiao, S.; Fang, L. *Proteomics* **2015**, *15*, 1819−1828.

(6) Ma, J.; Wu, L.; Li, Z.; Lu, Z.; Yin, W.; Nie, A.; Ding, F.; Wang, B.; Han, H. *Anal. Chem.* **2018**, *90*, 7415−7421.

(7) Heidari, R.; Rashidiani, J.; Abkar, M.; Taheri, R. A.; Moghaddam, M. M.; Mirhosseini, S. A.; Seidmoradi, R.; Nourani, M. R.; Mahboobi, M.; Keihan, A. H.; Kooshki, H. *Biosens. Bioelectron.* **2019**, *126*, 7−14.

(8) Jia, Y.; Liu, S.; Du, Y.; Yang, L.; Liu, X.; Liu, L.; Ren, X.; Wei, Q.; Ju, H. *Anal. Chem.* **2020**, *92*, 9179−9187.

(9) Khan, M. S.; Ameer, H.; Ali, A.; Li, Y.; Yang, L.; Ren, X.; Wei, Q. *Biosens. Bioelectron.* **2020**, *162*, 112235.

(10) Wang, C.; Han, Q.; Mo, F.; Chen, M.; Xiong, Z.; Fu, Y. *Anal. Chem.* **2020**, *92*, 12145−12151.

(11) Nie, Y.; Zhang, X.; Zhang, Q.; Liang, Z.; Ma, Q.; Su, X. *Biosens. Bioelectron.* **2020**, *160*, 112217.

(12) Liu, J.; Chen, P.; Xia, F.; Liu, Z.; Liu, H.; Yi, J.; Zhou, C. *Sens. Actuators, B* **2020**, *315*, 128098.

(13) Khoshfetrat, S. M.; Khoshsafar, H.; Afkhami, A.; Mehrgardi, M. A.; Bagheri, H. *Anal. Chem.* **2019**, *91*, 6383−6390.

(14) Shao, K.; Wang, B.; Nie, A.; Ye, S.; Ma, J.; Li, Z.; Lv, Z.; Han, H. *Biosens. Bioelectron.* **2018**, *118*, 160−166.

(15) Shao, K.; Wang, B.; Ye, S.; Zuo, Y.; Wu, L.; Li, Q.; Lu, Z.; Tan, X.; Han, H. *Anal. Chem.* **2016**, *88*, 8179−8187.

(16) Shao, K.; Zhang, C.; Ye, S.; Cai, K.; Wu, L.; Wang, B.; Zou, C.; Lu, Z.; Han, H. *Sens. Actuators, B* **2017**, *240*, 586−594.

(17) Wang, J.; Jiang, X.; Han, H. *Biosens. Bioelectron.* **2016**, *82*, 26−31.

(18) Wu, L.; Ding, F.; Yin, W.; Ma, J.; Wang, B.; Nie, A.; Han, H. *Anal. Chem.* **2017**, *89*, 7578−7585.

(19) Shao, K.; Wang, J.; Jiang, X.; Shao, F.; Li, T.; Ye, S.; Chen, L.; Han, H. *Anal. Chem.* **2014**, *86*, 5749−5757.

(20) Huang, B.; Yao, C.; Zhang, Y.; Lu, X. *Talanta* **2020**, *218*, 121126.

(21) Gao, T.-B.; Zhang, J.-J.; Wen, J.; Yang, X.-X.; Ma, H.-b.; Cao, D.-K.; Jiang, D. *Anal. Chem.* **2020**, *92*, 1268−1275.

(22) Ma, L.; Wu, N.; Liu, Y.; Ran, X.; Xiao, D. *Electrochim. Acta* **2019**, *297*, 826−832.

(23) Vinyard, D. J.; Su, S.; Richter, M. M. *J. Phys. Chem. A* **2008**, *112*, 8529−8533.

(24) Zhao, Y.; Zhang, Q.; Chen, K.; Gao, H.; Qi, H.; Shi, X.; Han, Y.; Wei, J.; Zhang, C. *J. Mater. Chem. C* **2017**, *5*, 4293−4301.

(25) Song, Y.; Zhang, W.; He, S.; Shang, L.; Ma, R.; Jia, L.; Wang, H. *ACS Appl. Mater. Interfaces* **2019**, *11*, 33676−33683.

(26) Zhang, W.; Song, Y.; He, S.; Shang, L.; Ma, R.; Jia, L.; Wang, H. *Nanoscale* **2019**, *11*, 20910−20916.

(27) Zhang, R.; Zhong, X.; Chen, A.-Y.; Liu, J.-L.; Li, S.-K.; Chai, Y.-Q.; Zhuo, Y.; Yuan, R. *Anal. Chem.* **2019**, *91*, 3681−3686.

(28) Miao, W. *Chem. Rev.* **2008**, *108*, 2506−2553.

(29) Zhao, Y.; Zhang, R.; Xu, Y.; Qi, H.; Chen, X.; Zhang, C. *J. Electroanal. Chem.* **2015**, *739*, 28−35.
(30) Tokel, N. E.; Keszthelyi, C. P.; Bard, A. J. *J. Am. Chem. Soc.* **1972**, *94*, 4872−4877.
(31) Zhang, Y.; Wang, F.; Liu, C.; Wang, Z.; Kang, L.; Huang, Y.; Dong, K.; Ren, J.; Qu, X. *ACS Nano* **2018**, *12*, 651−661.
(32) Wang, J.; Fan, Y.; Tan, Y.; Zhao, X.; Zhang, Y.; Cheng, C.; Yang, M. *ACS Appl. Mater. Interfaces* **2018**, *10*, 36615−36621.
(33) Goel, S.; Ferreira, C. A.; Chen, F.; Ellison, P. A.; Siamof, C. M.; Barnhart, T. E.; Cai, W. *Adv. Mater.* **2018**, *30*, 1704367.
(34) Peng, M.; Guan, G.; Deng, H.; Han, B.; Tian, C.; Zhuang, J.; Xu, Y.; Liu, W.; Lin, Z. *Environ. Sci.: Nano* **2019**, *6*, 207−215.
(35) Du, P.; Niu, Q.; Chen, J.; Chen, Y.; Zhao, J.; Lu, X. *Anal. Chem.* **2020**, *92*, 7980−7986.
(36) Kusior, A.; Banas, J.; Trenczek-Zajac, A.; Zubrzycka, P.; Micek-Ilnicka, A.; Radecka, M. *J. Mol. Struct.* **2018**, *1157*, 327−336.
(37) Yang, X.; Yu, Y.-Q.; Peng, L.-Z.; Lei, Y.-M.; Chai, Y.-Q.; Yuan, R.; Zhuo, Y. *Anal. Chem.* **2018**, *90*, 3995−4002.
(38) Yu, Z.; Wei, X.; Yan, J.; Tu, Y. *Analyst* **2012**, *137*, 1922−1929.
(39) Feng, D.; Chung, W.-C.; Wei, Z.; Gu, Z.-Y.; Jiang, H.-L.; Chen, Y.-P.; Darensbourg, D. J.; Zhou, H.-C. *J. Am. Chem. Soc.* **2013**, *135*, 17105−17110.
(40) Sohrabi, S.; Dehghanpour, S.; Ghalkhani, M. *J. Mater. Sci.* **2017**, *53*, 3624−3639.
(41) Ghazizadeh, A. J.; Afkhami, A.; Bagheri, H. *Mikrochim. Acta* **2018**, *185*, 296.
(42) Hashemi, P.; Afkhami, A.; Baradaran, B.; Halabian, R.; Madrakian, T.; Arduini, F.; Nguyen, T. A.; Bagheri, H. *Anal. Chem.* **2020**, *92*, 11405−11412.
(43) Li, L.; Ning, X.; Qian, Y.; Pu, G.; Wang, Y.; Zhang, X.; Wang, H.; Chen, J.; Shan, D.; Lu, X. *Sens. Actuators, B* **2018**, *257*, 331−339.
(44) Li, J.; Yang, L.; Luo, S.; Chen, B.; Li, J.; Lin, H.; Cai, Q.; Yao, S. *Anal. Chem.* **2010**, *82*, 7357−7361.
(45) Luo, D.; Huang, B.; Wang, L.; idris, A. M.; Wang, S.; Lu, X. *Electrochim. Acta* **2015**, *151*, 42−49.
(46) Wen, Y.; Luo, F.; Yang, Y.; Lin, L.; Du, J.; Guo, Y.; Xiao, D.; Choi, M. M. F. *Anal. Methods* **2012**, *4*, 1053−1059.
(47) Anouar, K.; Mansour, B. *Electrophoresis—Life Sciences Practical Applications*; Books on Demand, 2018; Vol. *8*, pp 125−146.
(48) Yuan, S.; Wang, J.; Wang, X.; Long, S.; Zhang, G.; Yang, J. *Polym. Eng. Sci.* **2015**, *55*, 2829−2837.
(49) Liufu, S.; Xiao, H.; Li, Y. *J. Colloid Interface Sci.* **2005**, *281*, 155−163.
(50) Fang, D.; Zheng, X.; Yi, H.; Dai, H.; Hong, Z.; Peng, Y.; Lin, Y. *Sens. Actuators, B* **2019**, *283*, 407−414.
(51) Tian, C.-Y.; Zhao, W.-W.; Wang, J.; Xu, J.-J.; Chen, H.-Y. *Analyst* **2012**, *137*, 3070−3075.
(52) Zhu, X.; Zhai, Q.; Gu, W.; Li, J.; Wang, E. *Anal. Chem.* **2017**, *89*, 12108−12114.
(53) Deng, S.; Ju, H. *Analyst* **2013**, *138*, 43−61.

https://dx.doi.org/10.1021/acs.analchem.0c03836
Anal. Chem. 2021, 93, 2090−2096